

## INVITED REVIEW

# Impact of the mouse estrus cycle on cannabinoid receptor agonist-induced molecular and behavioral outcomes

Hye Ji J. Kim<sup>1</sup> | Ayat Zagzoog<sup>1</sup> | Tallan Black<sup>1</sup> | Sarah L. Baccetto<sup>1</sup> | Udoka C. Ezeaka<sup>1</sup> | Robert B. Laprairie<sup>1,2</sup> 

<sup>1</sup>College of Pharmacy and Nutrition, University of Saskatchewan, Saskatoon, Saskatchewan, Canada

<sup>2</sup>Department of Pharmacology, College of Medicine, Dalhousie University, Halifax, Nova Scotia, Canada

## Correspondence

Robert B. Laprairie, College of Pharmacy and Nutrition, University of Saskatchewan, Health Sciences Bldg. Rm 3B36, 107 Wiggins Rd., Saskatoon, SK, Canada S7N 5E5.  
Email: robert.laprairie@usask.ca

## Funding information

This work was supported by the National Sciences and Engineering Research Council [Discovery Grant GECR-2019-00207]; and the College of Pharmacy and Nutrition at the University of Saskatchewan.

## Abstract

Sexual dimorphisms are observed in cannabinoid pharmacology. It is widely reported that female animals are more sensitive to the cataleptic, hypothermic, antinociceptive, and anti-locomotive effects of cannabinoid receptor agonists such as CP55,940. Despite awareness of these sex differences, there is little consideration for the pharmacodynamic differences within females. The mouse estrus cycle spans 4–5 days and consists of four sex hormone-mediated phases: proestrus, estrus, metestrus, and diestrus. The endocannabinoid system interacts with female sex hormones including  $\beta$ -estradiol, which may influence receptor expression throughout the estrus cycle. In the current study, sexually mature female C57BL/6 mice in either proestrus or metestrus were administered either 1 mg/kg i.p. of the cannabinoid receptor agonist CP55,940 or vehicle. Mice then underwent the tetrad battery of behavioral assays measuring catalepsy, internal body temperature, thermal nociception, and locomotion. Compared with female mice in metestrus, those in proestrus were more sensitive to the anti-nociceptive effects of CP55,940. A similar trend was observed in CP55,940-induced catalepsy; however, this difference was not significant. As for cannabinoid receptor expression in brain regions underlying antinociception, the spine tissue of proestrus mice that received CP55,940 exhibited increased expression of cannabinoid receptor type 1 relative to treatment-matched mice in metestrus. These results affirm the importance of testing cannabinoid effects in the context of the female estrus cycle.

## KEYWORDS

cannabinoid, cannabinoid receptor, endocannabinoid system, estrus cycle, mouse

**Abbreviations:** 2-AG, 2-arachidonoylglycerol; AEA, anandamide; CB1R, type 1 cannabinoid receptor; CB2R, type 2 cannabinoid receptor; FSH, follicle-stimulating hormone; i.p., intraperitoneally; LH, luteinizing hormone; OVX, ovariectomized; PAG, periaqueductal gray; THC,  $\Delta^9$ -tetrahydrocannabinol.

This is an open access article under the terms of the Creative Commons Attribution-NonCommercial License, which permits use, distribution and reproduction in any medium, provided the original work is properly cited and is not used for commercial purposes.

© 2022 The Authors. *Pharmacology Research & Perspectives* published by John Wiley & Sons Ltd, British Pharmacological Society and American Society for Pharmacology and Experimental Therapeutics.

## 1 | INTRODUCTION

Cannabinoids effect males and females differently, which has increasingly standardized the practice of including both sexes in pre-clinical research.<sup>1</sup> Despite these efforts, there is a general lack of consideration for the fluctuations of sex hormones within the sexes, particularly within females. Comparable with the 28-day human menstrual cycle, mice undergo a 4–5 day estrus cycle consisting of the following hormone-mediated phases: proestrus, estrus, metestrus, and diestrus.<sup>2</sup> Proestrus and estrus are characterized by elevated follicle-stimulating hormone (FSH), luteinizing hormone (LH), and  $\beta$ -estradiol, whereas metestrus and diestrus are marked by decreases in these hormones and an increase in circulating progesterone.<sup>2–5</sup> The estrus cycle influences aspects of the endocannabinoid system including cannabinoid receptor expression and function<sup>6–8</sup> as well as endocannabinoid concentrations.<sup>9</sup> Behavioral studies have also revealed that exogenous cannabinoids have different magnitudes of behavioral effects depending on the estrus cycle phase.<sup>10–12</sup> The current study provides molecular evidence to support the behavioral observations of these estrus cycle-mediated cannabinoid effects.

The estrus cycle influences endocannabinoid system functionality in a brain region-dependent manner. In the limbic forebrain—consisting of the hypothalamus, amygdala, and hippocampus—the density of the type 1 cannabinoid receptor (CB1R) does not change between cycle phases.<sup>6</sup> When it comes to binding potential, CB1R in these limbic regions have a higher affinity to cannabinoid ligands during diestrus compared with estrus.<sup>6</sup> In other studies involving ovariectomized (OVX) rats, hippocampal and hypothalamic CB1R display greater binding site density in OVX rats with lower circulating  $\beta$ -estradiol compared with normally cycling/non-OVX females.<sup>8</sup> Interestingly, the opposite binding pattern is seen in the amygdala.<sup>8</sup> Regarding the endocannabinoids, pituitary levels of 2-arachidonoylglycerol (2-AG) and anandamide (AEA) are higher during proestrus compared with late estrus and metestrus when circulating  $\beta$ -estradiol is relatively lower.<sup>9,13</sup> In the hypothalamus, both endocannabinoid levels are greater in diestrus compared with all other phases.<sup>9</sup> Endocannabinoid levels do not fluctuate in the striatum throughout the phases, while midbrain levels are more dependent on circulating progesterone compared with  $\beta$ -estradiol.<sup>9,13</sup> It remains unclear as to why each brain region is differentially affected by the interactions between the estrus cycle and endocannabinoid system.

Although administering exogenous cannabinoids to cycling females adds another layer of complexity to these dynamic brain region-specific interactions, these behavioral data provide valuable pharmacodynamic insights. For example, 5–10 mg/kg of  $\Delta^9$ -tetrahydrocannabinol (THC) induces greater paw pressure antinociception during estrus compared with diestrus when estrogen levels are relatively low.<sup>10,11</sup> Mice in estrus are also slightly more sensitive to the anti-locomotive and cataleptic effects of intraperitoneally (i.p.) injected THC, however, these differences are generally difficult to detect and largely depend on the route of administration.<sup>10</sup> These behavioral measures—along with body temperature,

commonly referred to as the tetrad battery of *in vivo* assays—are controlled by different brain regions. The differences in THC-induced antinociception between the estrus cycle phases indicate that regions such as the CB1R- and type 2 cannabinoid receptor (CB2R)-dense periaqueductal gray (PAG) and spine are the most affected by the fluctuations of female sex hormones.<sup>14,15</sup> To date, there are no published reports on how the estrus cycle influences CB1R and CB2R in the major brain regions that underlie these tetrad effects. This information is not only translatable to the use of cannabinoids by normally cycling human females but is also useful for preclinical research exploring the intricacies of the female endocannabinoid system.

## 2 | MATERIALS AND METHODS

### 2.1 | Compounds

CP55,940 was purchased from Cayman Chemical Company (Ann Arbor, MI, Cat # 90084) and was stored at  $-20^{\circ}\text{C}$  until use. The stock compound was dissolved in 100% methanol before being added to a vehicle solution consisting of 1:1:18 ethanol: Kolliphor EL (MilliporeSigma): 1 M phosphate-buffered saline (Fischer). The volume of vehicle added to the CP55,940 solution depended on the treatment dose and the mouse's body weight. CP55,940 was prepared at room temperature, then stored at  $4^{\circ}\text{C}$  for 10–15 min before use. The vehicle treatments were prepared at a constant volume of 200  $\mu\text{l}$ , then stored at  $4^{\circ}\text{C}$  for up to 10–15 min before injections commenced.

### 2.2 | Estrus cycle phase determination

All mice underwent estrus cycle phase determination between 08:00 and 10:00 each day. The published protocol by McLean et al.<sup>2</sup> was used to guide the following steps: (1) Vaginal lavage using a pipette to circulate 100  $\mu\text{l}$  of sterile ddH<sub>2</sub>O throughout the vaginal canal to collect a sample of vaginal epithelial and blood cells, (2) crystal violet staining of the mounted vaginal sample followed by two washes with ddH<sub>2</sub>O and cover-slipping with 15  $\mu\text{l}$  of glycerol; and (3) microscopic cytological determination of which estrus cycle phase the vaginal sample represented. A ZOE Cell Imager (Bio-Rad) was used to take photos of the stained vaginal samples. Proestrus was visually determined by the predominance of nucleated epithelial cells (>80%), which have an overall round shape containing a darkly stained nucleus.<sup>2,10,16</sup> The surge in circulating or plasma  $\beta$ -estradiol during proestrus causes hyperplastic and exfoliating responses in vaginal epithelial cells ahead of ovulation in the next cycle phase.<sup>17</sup> Metestrus was ruled by a combination of cornified squamous epithelial cells (~40%) and leukocytes (~60%).<sup>2,10,16</sup> The cornified squamous epithelial cells appear flattened, dried, and without a nucleus, whereas leukocytes are much smaller, rounder, and darkly stained.<sup>2,10,16</sup> This combination of terminally differentiated epithelial

cells and blood cells is associated with decreased  $\beta$ -estradiol levels and the continual rise in progesterone, which initiates the luteal phase following ovulation.<sup>2,17</sup> Thus, the fluctuations of these sex hormones, particularly  $\beta$ -estradiol, drive the cytological changes characteristics of the mouse estrus cycle.<sup>17</sup> Phase determination was further validated by an ELISA experiment measuring relative concentrations of  $\beta$ -estradiol in the plasma for each mouse.<sup>3-5</sup> The methodological details of the ELISA are explained in the following sections. Mice in either proestrus or metestrus proceeded to be injected and tested within 1 h of vaginal sample cytology.

### 2.3 | Animals and tetrad battery of in vivo assays

Sexually mature female C57BL/6 mice aged 6–12 weeks (mean weight:  $20 \pm 3$  g) were purchased from Charles River Labs. Mice were group housed (5 per cage) and maintained on a 12 h light:dark cycle (07:00–19:00/19:00–07:00), throughout which they had ad libitum access to food, water, and environmental enrichment. Depending on whether they were in proestrus or metestrus, mice were randomly designated to receive an i.p. injection of either 1 mg/kg CP55,940 or 200  $\mu$ l of the vehicle solution. One mg/kg CP55,940 was chosen based on a recent study by our group, which performed a dose-response experiment that included 5 i.p. doses of CP55,940 (0.1–3 mg/kg).<sup>18</sup> These earlier data revealed that 1 mg/kg i.p. CP55,940 evokes sub-maximal cataleptic, hypothermic, antinociceptive, and anti-locomotive responses in female mice of the same strain and age as the current study.<sup>18</sup> A lower dose of CP55,940 may not have produced significant catalepsy compared with the vehicle-treated group, while a higher dose would have caused maximal anti-locomotive effects or no movement in the open-field test.<sup>18</sup> Therefore, this sub-maximal response was chosen to determine in an attempt to detect estrus cycle-dependent fluctuations. The two estrus cycle phases and two treatment groups equaled four experimental groups with  $n = 4$  in the vehicle treatment group and  $n = 6$  in the 1 mg/kg CP55,940 treatment group. A total of 20 mice were used throughout the study. All protocols were in accordance with the guidelines detailed by the Canadian Council on Animal Care (CCAC, Ottawa ON: Vol. 1, 2nd Ed., 1993, Vol. 2, 1984) and approved by the Animal Research Ethics Board at the University of Saskatchewan. In keeping with the Animal Research: Reporting of In Vivo Experiments (ARRIVE) guidelines, power analyses were conducted to establish the minimum number of female mice required for the study. Additionally, mice were purchased, rather than bred, to limit animal waste.<sup>19</sup>

The tetrad battery of in vivo assays commenced 10 min after the i.p. injection. These assays were performed by a double-blinded researcher who (1) did not know what estrus cycle phase the mice were in, (2) was unaware of the treatments prepared for each mouse, and (3) did not inject the mice. First was the ring holding assay to measure catalepsy. For this assay, mice were placed on a ring apparatus such that their forepaws clasped the 5-mm ring positioned 5 cm above the testing platform surface. The length of time that the

mouse clasped the ring was recorded (s), as the trial was completed when the mouse either turned its head or body and made three consecutive attempts to escape or was immobile for more than 60 s [i.e., maximum possible effect (MPE) = 60 s]. Fifteen min following injections, a rectal thermometer was used to measure the injection-induced change in internal body temperature ( $^{\circ}$ C). Basal body temperature was recorded immediately prior to injections; therefore, the second temperature measurement allowed for calculating the change in body temperature ( $\Delta^{\circ}$ C). Twenty min post-injection, mice underwent the tail flick latency assay. In this assay, mice were restrained with their tails placed approximately 1 cm into  $52 \pm 2^{\circ}$ C water. The latency of time until the tail was removed from the water was recorded (s). Tails were removed after 20 s if they had not been removed already (i.e., MPE = 20 s). Finally, the open-field test was performed 25 min after injections. Mice were placed in a  $55 \times 55$  cm square-shaped open field for 10 min, during which they were free to roam. Distance travelled (m) and average velocity (cm/s) were scored with EthoVision XT (Noldus Information Technology Inc.). All tetrad scores were averaged between mice in the same experimental group to derive the means.<sup>18,20,21</sup> The means and standard errors of the means then underwent statistical processing.<sup>18,20,21</sup>

### 2.4 | Blood and brain tissue collection

Mouse blood and brain samples were collected approximately 45 min following injections between 10:00–12:00 on the day of testing. Mice were placed in a rodent induction chamber delivering a mixture of oxygen and isoflurane for approximately 2 min until the mouse was fully anaesthetized. Cardiac puncture was performed to collect approximately 0.5 ml of blood from each mouse. Blood was stored in BD Vacutainer™ Plastic Blood Collection Tubes with Lithium Heparin: Hemogard (Becton Dickinson) and kept on ice before being centrifuged at 3000g for 10 min at  $4^{\circ}$ C. The supernatant or plasma was collected and stored in  $-80^{\circ}$ C until further ELISA analysis. Immediately following cardiac puncture, mice were decapitated, and their brains were removed from the skull to dissect the following regions: PAG, spine, and hypothalamus. All brain region samples were kept on ice for up to 1.5 h before being flash-frozen in liquid nitrogen and stored at  $-80^{\circ}$ C until further use.

### 2.5 | $\beta$ -estradiol and protein quantification

Plasma collected from the cardiac puncture was retrieved from  $-80^{\circ}$ C storage and evaluated for  $\beta$ -estradiol content using the 17  $\beta$  Estradiol ELISA Kit (Abcam). The manufacturer's instructions were carefully followed and are summarized as follows: 25  $\mu$ l of each standard protein preparation (ranging from 0–2000 pg/ml) and each of the 20 experimental samples were added to their respective anti-17  $\beta$  estradiol IgG-coated wells. 200  $\mu$ l of 17  $\beta$  estradiol-HRP conjugate solution was also added to each occupied well, including the negative control wells. The microplate was incubated in  $37^{\circ}$ C for 2 h

protected from light. Following the incubation, the contents of the wells were aspirated then thoroughly washed with the manufacturer-provided washing solution. 100  $\mu$ l of 3,3',5,5'-tetramethylbenzidine substrate solution was then added to the wells and left to incubate in room temperature for 30 min protected from light. After these 30 min, 100  $\mu$ l of stop solution—intended to terminate the enzyme-substrate reaction—was added to the wells. The absorbance of the wells was measured using a Cytation5 plate reader (BioTek) set at an absorbance level of 450 nm.

For the brain homogenization and protein quantification steps, samples were constantly kept on ice and/or maintained at 4°C. Samples were homogenized in a lysis buffer solution consisting of 0.01  $\mu$ l HALT (Thermo Scientific) and 0.01  $\mu$ l EDTA (Thermo Scientific) per 1  $\mu$ l RIPA Lysis and Extraction Buffer (Thermo Scientific). Homogenized samples were then centrifuged at 11 000g for 10 min. The supernatant was collected, and the protein concentration was quantified using the Pierce™ BCA Protein Assay Kit (Thermo Scientific). The quantified proteins were quickly aliquoted then stored in -80°C until further SDS-PAGE and immunoblotting analysis. Plasma collected from the cardiac puncture was retrieved from -80°C storage and evaluated for  $\beta$ -estradiol content using the 17  $\beta$  Estradiol ELISA Kit (Abcam).

## 2.6 | SDS-PAGE and immunoblotting

Samples were diluted to their final concentrations in 2X Laemml sample buffer (Bio-Rad) containing 50  $\mu$ l of  $\beta$ -mercaptoethanol (Sigma-Aldrich), then boiled at 95°C for 10 min. For SDS-PAGE, 35  $\mu$ g of protein were loaded in each well of Novex™ WedgeWell™ 10%–20% tris-glycine polyacrylamide gels (Invitrogen). Protein-containing gels were then immersed in 25 mM of Tris-base, 190 mM of glycine, and 0.1% SDS (pH 7.4) and resolved at 125 V for 15 min, followed by 75 V for 1.5 h. Proteins were transferred to 0.45- $\mu$ m nitrocellulose membranes (Thermo Scientific) at 25 V for 2 h with transfer buffer containing 25 mM Tris-Base, 192 mM glycine, and 100 mM MeOH (pH 7.4) over ice in room temperature. Membranes were blocked for 1 h with tris-buffered saline (TBS) containing 20% Intercept Blocking Buffer (Li-Cor Biosciences) and 0.1% Triton X-100 (Sigma-Aldrich) at room temperature.

For immunoblotting, nitrocellulose membranes were incubated overnight at 4°C with the following primary antibodies: cannabinoid receptor CB1R monoclonal antibody (mouse, Synaptic Systems, Göttingen, Germany, Lot 1–3, Cat # 258011) diluted at 1:500, cannabinoid receptor CB2R polyclonal antibody (rabbit, Abcam, Cambridge, United Kingdom, Lot GR3411487-3, Cat # 3561) diluted at 1:250, and anti- $\beta$ -Actin antibody (MilliporeSigma, Oakville, Lot 50050902, Cat # SAB3500350) diluted at 1:1,500. Membranes were briefly rinsed with TBST (TBS containing Tween® 20) before undergoing three thorough washes with fresh TBST at room temperature: (1) one 30 min wash (2) three 5 min washes, and (3) one 10 min wash. Membranes were then incubated for 1 h at room temperature and protected from light with the following secondary antibodies: Goat

Anti-Mouse IgG H&L (Alexa Fluor® 594) (Invitrogen, Lot 2179228, Cat # A11005) diluted at 1:500 to tag the CB1R signal; Goat Anti-Rabbit IgG H&L (Alexa Fluor® 488) (Invitrogen, Lot 2179202, Cat # A11008) diluted at 1:500 to tag the CB2R signal; and Goat Anti-Chicken IgG H&L (Alexa Fluor® 680) (Invitrogen, Lot UB282080, Cat # A32934) diluted at 1:500 to tag the  $\beta$ -Actin signal. All primary and secondary antibodies were diluted in a solution of 20% Intercept Blocking Buffer, 0.1% Triton X-100, and 1 M TBS. Following the secondary antibody incubation, membranes underwent three more washes with TBST at room temperature as they were protected from light: (1) one 30-min wash, (2) three 5-min washes, and (3) one 10-min wash. Membranes were then quickly rinsed in double-distilled water before being visualized using the Bio-Rad ChemiDoc MP imaging system and software (17001402) (Bio-Rad). Densitometrical analysis was done via Image Lab 6.0 (Bio-Rad).

## 2.7 | Statistical analysis

Tetrad data are presented as a mean  $\pm$  SEM where “n” represents individual mice within treatment groups. Data from the ring holding assay and tail flick latency assay are reported as %MPE for catalepsy and %MPE for anti-nociception, respectively. Average velocity scores from the open-field test are presented as cm/s. Distance travelled scores from the open-field test are presented as m. SDS-PAGE data are calculated as adjusted total band volumes of optical densities (subtracted of background intensity) and presented as an expression of CB1R or CB2R over that of the housekeeping gene  $\beta$ -Actin. The raw ELISA data were collected as absorbance levels then converted and presented as pg/ml. Statistical analysis for all data from the tetrad, SDS-PAGE, and ELISA experiments were conducted by a two-way ANOVA to account for both the estrus cycle phase and treatment. Tukey's (two-way ANOVA) test was used for the post hoc analysis where significance was set at  $p < .05$ .

## 2.8 | Nomenclature of targets and ligands

Key protein targets and ligands in this article are hyperlinked to corresponding entries in <http://www.guidetopharmacology.org>, the common portal for data from the IUPHAR/BPS Guide to PHARMACOLOGY<sup>22</sup>, and are permanently archived in the Concise Guide to PHARMACOLOGY 2019/20.<sup>23</sup>

## 3 | RESULTS

### 3.1 | Tetrad battery of in vivo assays

Female mice in proestrus and metestrus were treated with either 1 mg/kg CP55,940 or a vehicle solution before undergoing the tetrad battery of assays. Within the proestrus groups, mice treated with 1 mg/kg of CP55,940 displayed greater catalepsy compared with

their vehicle counterparts ( $p < .01$ ) (Figure 1A). There were no significant differences in catalepsy between the vehicle- and CP55,940-treated metestrus mice nor were there clear CP55,940-mediated catalepsy differences between the estrus cycle phases (Figure 1A). In contrast to metestrus, proestrus accentuated the cataleptic effect of CP55,940 (Figure 1A). Regarding internal body temperature, 1 mg/kg CP55,940 induced hypothermia in both estrus cycle phases ( $p < .001$ ) (Figure 1B). There were no significant body temperature differences detected between proestrus and metestrus mice that received 1 mg/kg of CP55,940 (Figure 1B). These results indicated that 1 mg/kg CP55,940 similarly affected the internal body temperature of both phases (Figure 1B). For antinociception, 1 mg/kg CP55,940 significantly increased thermal antinociception in proestrus mice only ( $p < .001$ ) (Figure 1C). Compared with metestrus mice, those in proestrus were also more sensitive to the antinociceptive effects of 1 mg/kg CP55,940 ( $p < .01$ ) (Figure 1C). Finally, 1 mg/kg CP55,940 caused metestrus mice to travel less distance ( $p < .001$ ) (Figure 1D) at a lower average velocity ( $p < .01$ ) (Figure 1E) in the open-field test compared with their vehicle counterparts. 1 mg/kg CP55,940 decreased both locomotion measures ( $p < .01$ ) (Figure 1D,E) in proestrus mice compared with their vehicle counterparts. Unlike the tail flick latency assay results, there were no differences between

the estrus cycle phases with respect to CP55,940-induced antinociception (Figure 1D,E). Thus, antinociception was the only tetrad measure in which 1 mg/kg of CP55,940 had contrasting effects between proestrus and metestrus (Figure 1C).

### 3.2 | ELISA

Prior to organizing the mice into their respective experimental groups, vaginal cytology was performed to identify which mice were in proestrus and metestrus (Figure 2A). The vaginal samples of proestrus mice exhibited a predominance of nucleated epithelial cells (<80%), while the samples of mice in metestrus consisted of both cornified squamous epithelial cells (~40%) and leukocytes (~60%) (Figure 2A). Once the tetrad battery of assays was completed (approximately 1.75 h following vaginal cytology and 45 min post-injections), blood was collected and used to measure  $\beta$ -estradiol levels. The plasma of vehicle-treated proestrus mice contained slightly higher concentrations of  $\beta$ -estradiol compared with vehicle-treated mice in metestrus; however, this difference was not statistically significant ( $p > .34$ ) (Figure 2B). Due to the timing of blood collection (after the injections), the ELISA results from the

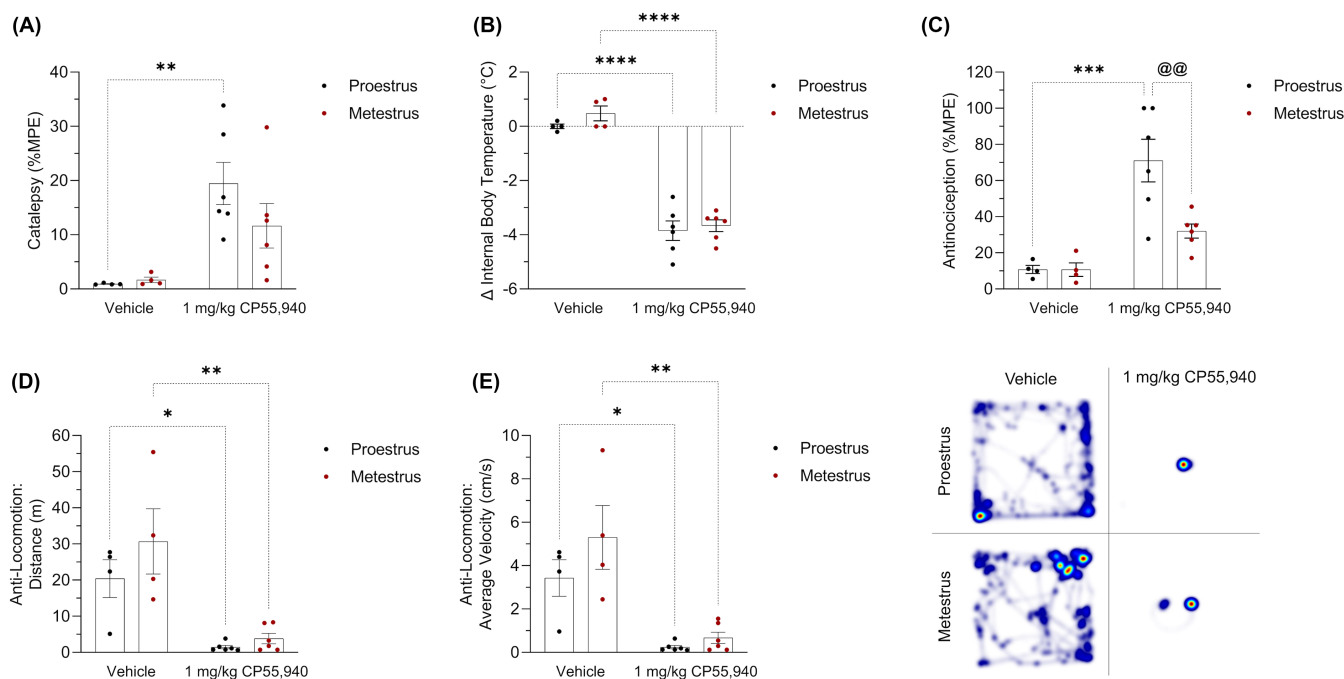


**FIGURE 1** Acute tetrad effects in female mice following treatment with CP55,940. Female C57BL/6 mice aged 6–12 weeks in either proestrus or metestrus were administered either 1 mg/kg CP55,940 or a vehicle solution i.p. (A) 10 min following the injections, mice underwent the ring holding assay to measure their cataleptic response. All catalepsy data are expressed as %MPE (MPE = 60 s). (B) 15 min post injections, a rectal thermometer was used to measure internal body temperature. Temperatures are recorded as °C. (C) 20 min after injections, thermal antinociception was measured using the tail flick latency assay. Latencies are presented as %MPE (MPE = 20 s). 25 min following injections, mice were placed in the open-field test evaluating treatment-induced locomotion. (D) Distance travelled is reported in m. (E) Average velocity is recorded in cm/s. (F) Representative heat map images illustrating locomotion in the open-field test. (A–E) Each dot on the graphs represent individual mice or  $n$ . Bars on the graphs indicate means  $\pm$  SEM, where  $n = 4$  (vehicle) and  $n = 6$  (1 mg/kg CP55,940). All means were compared between 1 mg/kg CP55,940 and vehicle groups within estrus cycle phases, as well as between proestrus and metestrus groups within treatments. Significance was calculated using a two-way ANOVA followed by Tukey's post hoc analyses. \*/\*\*/\*\*\*/\*\*\*\* $p < .05/.01/.001/.0001$  compared with vehicle within estrus cycle phase. @@ $p < .01$  compared with proestrus within treatment

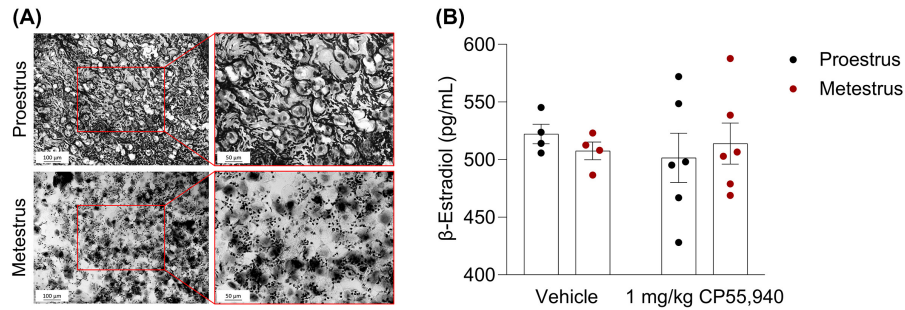


**FIGURE 2** Estrus cycle phase determination. (A) Representative light microscopy images of vaginal samples from vehicle-treated female mice in either proestrus or metestrus. A lavage of ddH<sub>2</sub>O collected loose epithelial and blood cells within the vaginal canal the female mice. The majority of cells (>80%) in the proestrus sample are nucleated epithelial cells that are round in shape and contain a pigmented nucleus at the center. The metestrus sample contains a combination of un-nucleated cornified squamous epithelial cells (~40%) and much smaller, darkly stained leukocytes (~60%). These different cell types and morphologies indicate estrus cycle-driven sex hormone fluctuations, especially that of  $\beta$ -estradiol. (B)  $\beta$ -estradiol ELISA results validating phase determination of vehicle- and CP55,940-treated groups. Immediately following the tetrad battery of behavioral assays, blood was collected from all mice. Plasma was measured for circulating  $\beta$ -estradiol content. Each point on the graph constitutes individual mice or *n*. Bars on the graph illustrate means  $\pm$  SEM, where *n* = 4–6 mice/group. A paired *t*-test determined no significant difference between the groups

1 mg/kg CP55,940-treated groups reflect ligand-induced confounds that were not observed in the vehicle-treated groups (Figure 2B).

### 3.3 | SDS-PAGE and immunoblotting

Brain tissue collected from the spine, PAG, and hypothalamus were evaluated for their expression of CB1R and CB2R. Within the spine of proestrus mice, 1 mg/kg of CP55,940 increased the expression of CB1R ( $p < .05$ ) (Figure 3A). This cannabinoid-induced difference in CB1R expression was not observed in the spine of metestrus mice ( $p > .05$ ) (Figure 3A). When comparing between the spine tissue of proestrus and metestrus mice treated with 1 mg/kg CP55,940, the spine of cannabinoid-treated proestrus mice displayed greater CB1R expression compared (Figure 3A). No treatment- nor estrus cycle phase-dependent differences were observed in spine CB2R expression (Figure 3B). No significant differences in cannabinoid receptor expression were observed in the PAG (Figure 3D–F). Within the hypothalamus, proestrus mice treated with 1 mg/kg of CP55,940 had increased CB1R expression compared with cycle phase-matched mice that received the vehicle solution (Figure 3G). No other differences were observed in the hypothalamus (Figure 3G,H). Representative images of these data are provided in Figure 3C,F,I. The only estrus cycle phase-dependent difference was observed with regards to CB1R expression in the spine (Figure 3A).

## 4 | DISCUSSION

The current study aimed to assess varying cannabinoid effects across the female menstrual or estrus cycle. Throughout the last decade, several groups have tested cannabinoids in female rodents occupying different estrus cycle phases; some reporting noteworthy differences in tetrad effects based on the cannabinoid tested and its route

of administration. For instance, 5–10 mg/kg of i.p. THC has greater antinociceptive effects during estrus and proestrus when estrogen levels are high, relative to diestrus and metestrus when levels are low.<sup>10,11</sup> In another more recent paper, neither 12.5–200 mg/ml of inhaled THC or 100–400 mg/ml inhaled cannabidiol (CBD) induced stronger antinociceptive effects in estrus compared with diestrus.<sup>24</sup> Unlike the current study's use of CP55,940, these groups administered THC, a partial agonist at both cannabinoid receptors, and/or CBD, a more ambiguous ligand with stronger affinities to various other receptor targets beyond the cannabinoid receptors.<sup>20,25–31</sup> Although studies involving the phytocannabinoids are more translatable given their recreational and medical accessibility, the current study's use of CP55,940, a full cannabinoid receptor agonist, provides a more straightforward scenario for delineating the complex interactions between the endocannabinoid system and fluctuating female sex hormones.

To determine the pharmacodynamics of exogenous cannabinoids in the context of the estrus cycle, one must first consider the underlying presence of endocannabinoids. The main endocannabinoids, 2-arachidonoylglycerol (2-AG) and anandamide (AEA) serve distinct binding functions and exist in varying concentrations throughout the brain. The estrus cycle and its associated fluctuations in circulating<sup>2–4</sup> and brain levels of  $\beta$ -estradiol<sup>32</sup> likely affect these endocannabinoid patterns. In rats, there are no endocannabinoid concentration differences between cycle phases in the striatum.<sup>9</sup> In the hypothalamus, both 2-AG and AEA levels are higher during diestrus—when circulating  $\beta$ -estradiol is relatively low—compared with the other phases.<sup>9</sup> In the midbrain consisting of the PAG, both endocannabinoid concentrations are largest during proestrus relative to most other phases.<sup>9</sup> Given these dynamic patterns, we must also acknowledge that CP55,940 is an orthosteric agonist that competes with the endocannabinoids to non-selectively bind to CB1R and CB2R.<sup>33</sup> In the current study, the brain regions modulating antinociception were more sensitive to 1 mg/kg of CP55,940 during proestrus compared

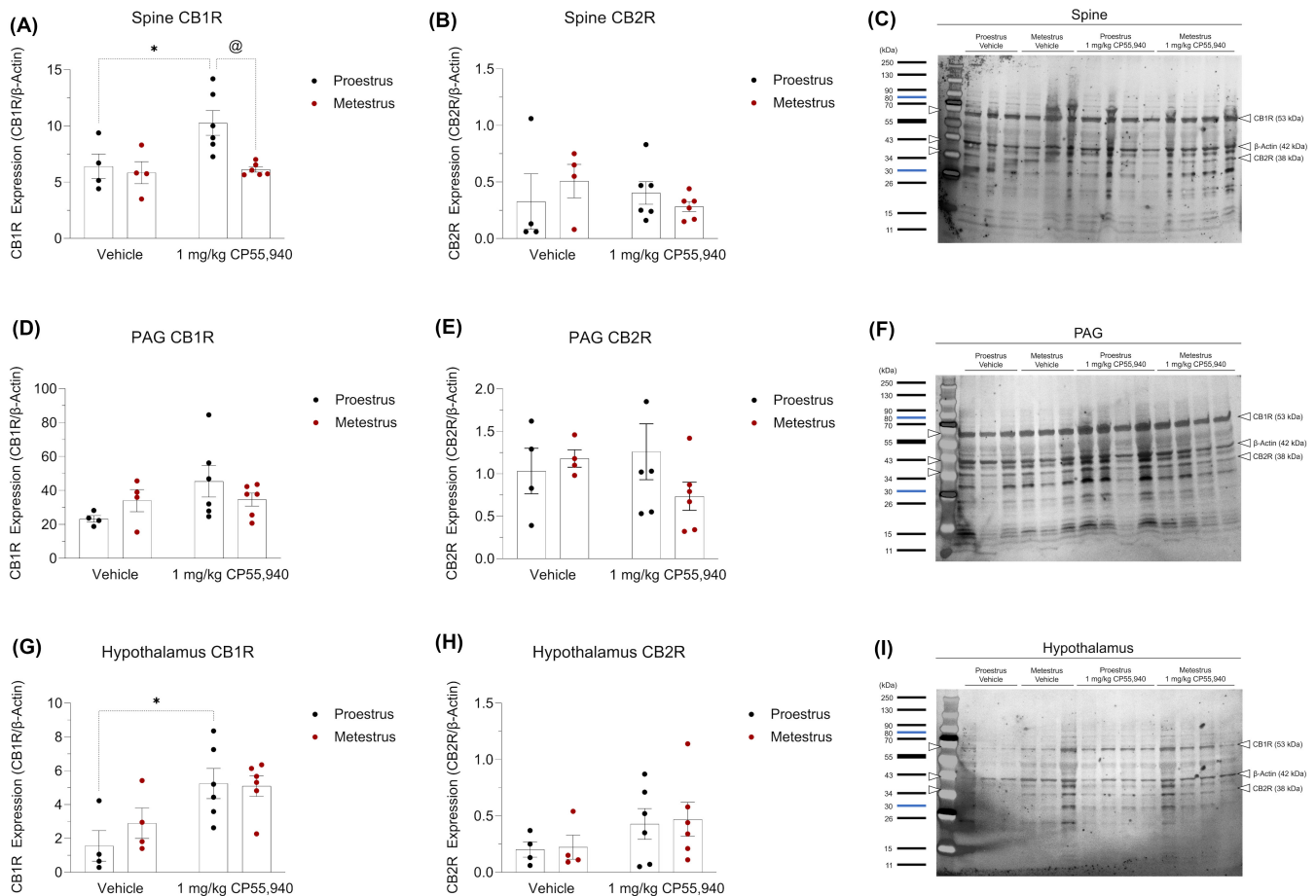


**FIGURE 3** Expression of cannabinoid receptors in brain regions underlying cannabinoid-induced thermal antinociception and hypothermia. SDS-PAGE and immunoblotting were performed on (A–C) spine, (D–F) PAG, and (G–I) hypothalamus tissue to quantify their optical density of the cannabinoid receptors. (A, D, G) CB1R expression of region-specific experimental groups. (B, E, H) CB2R expression of region-specific experimental groups. (C, F, I) Representative images of the region-specific CB1R, CB2R, and  $\beta$ -Actin bands identified using a ladder. (A–I)  $\beta$ -Actin was used as the housekeeping gene to normalize all cannabinoid receptor densities. Data is reported as ratios of adjusted total band volumes of optical densities. Each point on the graphs represent individual mice or  $n$ . Bars on the graphs illustrate means  $\pm$  SEM, where  $n = 4$  (vehicle) and  $n = 6$  (1 mg/kg CP55,940). All means were compared between 1 mg/kg CP55,940 and vehicle groups within estrus cycle phases, as well as between proestrus and metestrus groups within treatments. A two-way ANOVA followed by Tukey's post hoc analyses were used to determine significance. \* $p < .05$  compared with vehicle within estrus cycle phase. @ $p < .05$  compared with proestrus within treatment

with metestrus (Figure 3A). Although Bradshaw and colleagues<sup>9</sup> did not measure phase-mediated endocannabinoid levels in the spine, it may be that during proestrus, CP55,940 out-competes the endocannabinoids in the spine to activate the cannabinoid receptors.<sup>34,35</sup>

Similar to the endocannabinoids, the expression and function of the cannabinoid receptors also changes throughout the estrus cycle in a brain region-dependent manner. In the hypothalamus and hippocampus, cannabinoid receptor density and binding negatively correlate to circulating  $\beta$ -estradiol.<sup>6,8</sup> Other limbic regions such as the amygdala demonstrate the opposite pattern of increased cannabinoid receptor functionality in estrus cycle phases or experimental conditions where  $\beta$ -estradiol levels are high.<sup>8</sup> In the spine—a major region mediating thermal antinociception<sup>36</sup>—the administration of 1 mg/kg of CP55,940 led to a higher degree of CB1R immunolabelling during proestrus compared with metestrus (Figure 3A).

In agreement with the tetrad results, these phase-dependent differences were not detected in the hypothalamus, a region that regulates body temperature (Figures 1B and 3A).<sup>37,38</sup> These data suggest that the estrus cycle's influence on CB1R activation and subsequent upregulation in total CB1R protein quantity is most detectable in the spine (Figure 3A). Whether this receptor upregulation indicates de novo synthesis of proteins or post-translational reorganization of receptor expression on the plasma membrane remains unknown.<sup>39,40</sup> Furthermore, upregulated CB1R quantity does not necessarily point to increased receptor functionality as immunoblotting cannot distinguish between vesicle-enveloped and membrane-embedded receptors.<sup>39,40</sup> In the hypothetical case that Figure 3A's result does correspond to increased CB1R function, this may either be due to pre-existing distribution of receptors between brain regions<sup>41</sup> or region-specific availability of cannabinoid ligands.

Other neuromodulators in the spine such as endogenous opioids may also precipitate additive or synergistic signaling effects during proestrus.<sup>42,43</sup>

All these observations call into question the roles of circulating hormones during the estrus cycle on the endocannabinoid system. Although there is no clear evidence of endogenous estrogens binding to the cannabinoid receptors, exogenous estradiol benzoate has been shown to increase CB1R binding at GABAergic synapses of the hypothalamic arcuate nucleus, while having the inverse effect at glutamatergic synapses.<sup>44</sup> In another study,  $\beta$ -estradiol activity at hippocampal estrogen receptors led to AEA release, which retroactively inhibited presynaptic GABA release resulting in the excitation of postsynaptic pyramidal neurons.<sup>45</sup> In both experiments, estrogen enhanced CB1R-mediated GABAergic disinhibition.<sup>44,45</sup> What this entails for larger-scale receptor binding and expression remains unclear. Compared with the hippocampal CB1R of OVX females, CB1R of normally cycling females—with higher circulating  $\beta$ -estradiol—display an increased affinity for CP55,940 despite decreased binding site density.<sup>8</sup> We observed that circulating  $\beta$ -estradiol was positively—although non-significantly—associated with sensitivity to CP55,940-induced antinociception. Therefore, our data may represent a scenario in which the spinal antinociceptive effects of CP55,940 intensify during proestrus in correlation with  $\beta$ -estradiol.<sup>8,44</sup> Unfortunately, the literature supporting this theory focuses on the hypothalamus and hippocampus, whereas our most significant observations pertained to spinal function.

The current study serves as a point of entry in the female endocannabinoid system. Beyond  $\beta$ -estradiol, other female sex hormones such as LH, FSH, and prolactin are also subject to fluctuations throughout the estrus and menstrual cycles of rodents and female humans, respectively. Another limitation of the current study design is the lack of gonadectomized females. Experimentation in this field often includes gonadectomized control groups to distinguish between (a) organization sex hormone effects derived from sexual [organ] development and (b) activation sex hormone effects triggered by the adult hypothalamic-pituitary-gonadal axis.<sup>10,46</sup> In the current study, plasma  $\beta$ -estradiol may be gonadal and/or brain-derived, both of which influence estrogenic neuromodulation.<sup>47</sup> Accurately determining estrus cycle phase in rodents proves difficult due to methodological limitations. A myriad of environmental confounds (e.g. light:dark cycle, feeding, drinking, and stress) may alter this rapidly cycling 4–5-day phase schedule.<sup>46</sup> Although our ELISA experiment did not yield significant differences between proestrus and metestrus groups (Figure 2B), future studies should continue to quantify circulating and locally derived sex hormones—while also noting the time of day of sample collection—to support their vaginal cytology.<sup>48</sup>

The motivation for the current study was to explain the variations within female tetrad data<sup>18</sup>; identify novel research questions pertaining to the female endocannabinoid system; and provide suggestions on how to conduct more intentional and better-controlled research on female subjects. Next steps to the current dataset

entail delineating the mechanisms of CB1R upregulation (e.g., de novo synthesis or post-translational reorganization) in the context of the estrus cycle.<sup>39,40</sup> Using polyestrous animals with longer reproductive or estrus phases will allow researchers to test different administration schedules (i.e., prolonged or chronic) and sample collection times to gain more precise information on these receptor upregulation mechanisms. These experimental factors could not be applied in the current study design as female mice cycle very quickly through the estrus cycle, sometimes transitioning into the next phase before the end of testing in the initial phase.<sup>46</sup> Aside from these molecular considerations, there are two directions that preclinical work focused on females can take that (1) the study can isolate each of the estrus cycle phases, or more simply differentiate between estrus-proestrus and diestrus-metestrus or (2) the study can include equal representation of all the cycle phases. However, there is growing consideration for the efficacy and safety of neuropsychotropic drugs in the context of menstrual cycles and hormone replacement and/or contraceptive therapies,<sup>49,50</sup> not to mention recent advancements in technology that enable women to track their menstrual cycles with accuracy and ease to make life decisions.<sup>51</sup> These reasons, along with equally important societal and biomedical discussions around sex and gender, warrant effort to delineate how cannabinoids interact with female sex hormones in whole body systems.

## ACKNOWLEDGMENTS

We thank the lab of Dr. John Howland at the University of Saskatchewan for lending us their light microscope to aid in the estrus cycle phase determination.

## DISCLOSURE

The authors declare that the research was conducted in the absence of any commercial or financial relationships that could be construed as a potential conflict of interest.

## AUTHOR CONTRIBUTIONS

*Participated in research design:* Kim and Laprairie. *Conducted the experiments:* Kim, Zagzoog, Black, Baccetto, and Ezeaka. *Contributed new reagents or analytic tools:* Kim, Zagzoog, Black, Baccetto, Ezeaka, and Laprairie. *Performed data analysis:* Kim, Zagzoog, Black, Baccetto, Ezeaka, and Laprairie. *Wrote or contributed to the writing of the manuscript:* Kim and Laprairie.

## ETHICS STATEMENT

All animal use was in accordance with the guidelines detailed by the Canadian Council on Animal Care and approved by the Animal Research Ethics Board (AREB) at the University of Saskatchewan (Protocol number 20170099). In keeping with the Animal Research: Reporting of In Vivo Experiments (ARRIVE) guidelines, power analyses were conducted to establish the minimum number of female mice required for the study. Additionally, mice were purchased, rather than bred, to limit animal waste.



## DATA AVAILABILITY STATEMENT

The data that support the findings of this study—including all images and recordings—are available from the corresponding author upon reasonable request.

## ORCID

Robert B. Laprairie  <https://orcid.org/0000-0002-9994-433X>

## REFERENCES

- Cooper ZD, Craft RM. Sex-dependent effects of cannabis and cannabinoids: a translational perspective. *NPP*. 2018;43:34-51.
- McLean AC, Valenzuela N, Fai S, Bennett SA. Performing vaginal lavage, crystal violet staining, and vaginal cytological evaluation for mouse estrous cycle staging identification. *J Vis Exp*. 2012;67:4389.
- Butcher RL, Collins WE, Fugo NW. Plasma concentration of LH, FSH, prolactin, progesterone and estradiol-17beta throughout the 4-day estrous cycle of the rat. *Endocrinology*. 1974;94:1704-1708.
- Walmer DK, Wrona MA, Hughes CL, Nelson KG. Lactoferrin expression in the mouse reproductive tract during the natural estrous cycle: correlation with circulating estradiol and progesterone. *Endocrinology*. 1992;131:458-1466.
- Miller BH, Takahashi JS. Central circadian control of female reproductive function. *Front Endocrinol*. 2014;4:195.
- Rodríguez de Fonseca F, Cebeira M, Ramos JA, Martín M, Fernández-Ruiz JJ. Cannabinoid receptors in rat brain areas: sexual differences, fluctuations during estrous cycle and changes after gonadectomy and sex steroid replacement. *Life Sci*. 1994;54:159-170.
- González S, Bisogno T, Wenger T, et al. Sex steroid influence on cannabinoid CB(1) receptor mRNA and endocannabinoid levels in the anterior pituitary gland. *Biochem Biophys*. 2000;270:260-266.
- Riebe CJ, Hill MN, Lee TT, Hillard CJ, Gorzalka BB. Estrogenic regulation of limbic cannabinoid receptor binding. *Psychoneuroendocrinology*. 2010;35:1265-1269.
- Bradshaw HB, Rimmerman N, Krey JF, Walker JM. Sex and hormonal cycle differences in rat brain levels of pain-related cannabinoid mimetic lipid mediators. *Am J Physiol Regul*. 2006;291:349-358.
- Craft RM, Leidl MD. Gonadal hormone modulation of the behavioral effects of Delta9-tetrahydrocannabinol in male and female rats. *Eur J Pharmacol*. 2008;578:37-42.
- Wakley AA, Craft RM. Antinociception and sedation following intracerebroventricular administration of  $\Delta^9$ -tetrahydrocannabinol in female vs. male rats. *Behav Brain Res*. 2011;216:200-206.
- Wakley AA, Wiley JL, Craft RM. Sex differences in antinociceptive tolerance to delta-9-tetrahydrocannabinol in the rat. *Drug Alcohol Depend*. 2014;143:22-28.
- Freeman ME. The neuroendocrine control of the ovarian cycle of the rat. In: Knobil E, Neill JD, eds. *The physiology of reproduction*. Raven Press; 1994:613-658.
- Lichtman AH, Martin BR. Spinal and supraspinal components of cannabinoid-induced antinociception. *JPET*. 1991;258:517-523.
- Lichtman AH, Cook SA, Martin BR. Investigation of brain sites mediating cannabinoid-induced antinociception in rats: evidence supporting PAG involvement. *JPET*. 1996;276:585-593.
- Cora MC, Kooistra L, Travlos G. Vaginal cytology of the laboratory rat and mouse: review and criteria for the staging of the estrous cycle using stained vaginal smears. *Toxicol Pathol*. 2015;43:776-793.
- Bertolin K, Murphy BD. Reproductive tract changes during the mouse estrous cycle. In: Croy BA, Yamada AT, DeMayo FJ, Adamson SL, eds. *The Guide to Investigation of Mouse Pregnancy*. Press; 2014:85-94.
- Kim HJJ, Zagzoog A, Smolyakova AM, et al. In vivo evidence for brain region-specific molecular interactions between cannabinoid and orexin receptors. *Front Neurosci*. 2021;15:790546.
- Kilkenny C, Browne WJ, Cuthill IC, Emerson M, Altman DG. Improving bioscience research reporting: the arrive guidelines for reporting animal research. *PLoS Biol*. 2010;8:1000412.
- Zagzoog A, Mohamed KA, Kim HJJ, et al. In vitro and in vivo pharmacological activity of minor cannabinoids isolated from *Cannabis sativa*. *Sci Rep*. 2020;10:20405.
- Zagzoog A, Brandt AL, Black T, et al. Assessment of select synthetic cannabinoid receptor agonist bias and selectivity between the type 1 and type 2 cannabinoid receptor. *Sci Rep*. 2021;11:10611.
- Harding SD, Sharman JL, Faccenda E, et al. The IUPHAR/BPS Guide to PHARMACOLOGY in 2019: updates and expansion to encompass the new guide to IMMUNOPHARMACOLOGY. *Nucleic Acids Res*. 2018;46:D1091-D1106.
- Alexander SPH, Christopoulos A, Davenport AP, et al. The concise guide to pharmacology 2019/20: G protein-coupled receptors. *Br J Pharmacol Suppl*. 2019;1:S21-S141.
- Javadi-Paydar M, Nguyen JD, Kerr TM, et al. Effects of  $\Delta^9$ -THC and cannabidiol vapor inhalation in male and female rats. *Psychopharmacology*. 2018;235:2541-2557.
- Esposito G, Scuderi C, Valenza M, et al. Cannabidiol reduces A $\beta$ -induced neuroinflammation and promotes hippocampal neurogenesis through PPAR $\gamma$  involvement. *PLoS One*. 2011;6:28668.
- Kathmann M, Flau K, Redmer A, Tränkle C, Schlicker E. Cannabidiol is an allosteric modulator at mu- and delta-opioid receptors. *Naunyn Schmiedebergs Arch Pharmacol*. 2006;372:354-361.
- Pertwee RG. The diverse CB1 and CB2 receptor pharmacology of three plant cannabinoids: delta9-tetrahydrocannabinol, cannabidiol and delta9-tetrahydrocannabivarin. *Br J Pharmacol*. 2008;153:199-215.
- Ahrens J, Demir R, Leuwer M, et al. The nonpsychotropic cannabinoid cannabidiol modulates and directly activates alpha-1 and alpha-1-beta glycine receptor function. *Pharmacology*. 2009;83:21.
- Scuderi C, Steardo L, Esposito G. Cannabidiol promotes amyloid precursor protein ubiquitination and reduction of beta amyloid expression in SHSY5YAPP+ cells through PPAR $\gamma$  involvement. *Phytother Res*. 2014;28:1007.
- Laprairie RB, Bagher AM, Kelly ME, Denovan-Wright EM. Cannabidiol is a negative allosteric modulator of the cannabinoid CB1 receptor. *Br J Pharmacol*. 2015;172:4790-4805.
- Tham M, Yilmaz O, Alaverdashvili M, Kelly M, Denovan-Wright EM, Laprairie RB. Allosteric and orthosteric pharmacology of cannabidiol and cannabidiol-dimethylheptyl at the type 1 and type 2 cannabinoid receptors. *Br J Pharmacol*. 2019;176:1455-1469.
- Woolley CS, McEwen BS. Estradiol mediates fluctuation in hippocampal synapse density during the estrous cycle in the adult rat. *J Neurosci*. 1992;12:2549-2554.
- Manning JJ, Green HM, Glass M, Finlay DB. Pharmacological selection of cannabinoid receptor effectors: signalling, allosteric modulation and bias. *Neuropharmacology*. 2021;193:108611.
- Ligresti A, De Petrocellis L, Di Marzo V. From phytocannabinoids to cannabinoid receptors and endocannabinoids: pleiotropic physiological and pathological roles through complex pharmacology. *Physiol Rev*. 2016;96:1593-1659.
- Howlett AC, Abood ME. CB1 and CB2 receptor pharmacology. *Adv Pharmacol*. 2017;80:169-206.
- Palazzo E, Luongo L, Novellis V, Rossi F, Maione S. The role of cannabinoid receptors in the descending modulation of pain. *Pharmaceuticals (Basel)*. 2010;3:2661-2673.
- Wenger T, Moldrich G. The role of endocannabinoids in the hypothalamic regulation of visceral function. *Prostaglandins Leukot Essent Fatty Acids*. 2002;66:301-307.
- Rawls SM, Cabassa J, Geller EB, Adler MW. CB1 receptors in the preoptic anterior hypothalamus regulate WIN 55212-2 [(4,5-dihydro-2-methyl)-4(4-morpholinylmethyl)-1-(1-naphthalenyl)-carbonyl

- l)-6H-pyrrolo[3,2,1ij]quinolin-6-one]-induced hypothermia. *JPET*. 2002;301:963-968.
39. Fletcher-Jones A, Hildick KL, Evans AJ, Nakamura Y, Henley JM, Wilkinson KA. Protein interactors and trafficking pathways that regulate the cannabinoid type 1 receptor (CB1R). *Front Mol Neurosci*. 2020;13:108.
  40. Irving AJ, McDonald NA, Harkany T. CB1 cannabinoid receptors: molecular biology, second messenger coupling and polarized trafficking in neurons. In: Köfalvi A, ed. *Cannabinoids and the Brain*. Springer; 2008:59-73.
  41. Mackie K. Distribution of cannabinoid receptors in the central and peripheral nervous system. *Handb Exp Pharmacol*. 2005;168:299-325.
  42. Fields HL, Basbaum AI, Heinricher MM. Central nervous systems mechanisms of pain modulation. In: McMahon SB, Koltzenburg M, eds. *Textbook of pain*. Elsevier; 2006:125-142.
  43. Tuboly G, Meccs L, Benedek G, Horvath G. Antinociceptive interactions between anandamide and endomorphin-1 at the spinal level. *Clin Exp Pharmacol Physiol*. 2009;36:400-405.
  44. Nguyen QH, Wagner EJ. Estrogen differentially modulates the cannabinoid-induced presynaptic inhibition of amino acid neurotransmission in proopiomelanocortin neurons of the arcuate nucleus. *Neuroendocrinology*. 2006;84:123-137.
  45. Huang GZ, Woolley CS. Estradiol acutely suppresses inhibition in the hippocampus through a sex-specific endocannabinoid and mGluR-dependent mechanism. *Neuron*. 2012;74:801-808.
  46. Becker JB, Arnold AP, Berkley KJ, et al. Strategies and methods for research on sex differences in brain and behavior. *Endocrinology*. 2005;146:1650-1673.
  47. Cornil CA, Ball GF, Balthazart J. Functional significance of the rapid regulation of brain estrogen action: where do the estrogens come from? *Brain Res*. 2006;1126:2-26.
  48. Weixelbaumer KM, Drechsler S, Wehrenpfennig P, et al. Estrus cycle status defined by vaginal cytology does not correspond to fluctuations of circulating estrogens in female mice. *Shock*. 2014;41:145-153.
  49. Bourne C, Kenkel L. Treatment of depression in women. *Handb Exp Pharmacol*. 2019;250:371-387.
  50. Yum SK, Yum SY, Kim T. The problem of medicating women like the men: conceptual discussion of menstrual cycle-dependent psychopharmacology. *Transl Clin Pharmacol*. 2019;27:127-133.
  51. Kressbach M. Period hacks: menstruating in the big data paradigm. *Telev New Media*. 2021;22:241-261.

#### SUPPORTING INFORMATION

Additional supporting information may be found in the online version of the article at the publisher's website.

**How to cite this article:** Kim HJJ, Zagzoog A, Black T, Baccetto SL, Ezeaka UC, Laprairie RB. Impact of the mouse estrus cycle on cannabinoid receptor agonist-induced molecular and behavioral outcomes. *Pharmacol Res Perspect*. 2022;10:e00950. doi:[10.1002/prp2.950](https://doi.org/10.1002/prp2.950)